DOI: 10.1111/j.1570-7458.2010.00983.x

New structure in cell puncture activities by aphid stylets: a dual-mode EPG study

W. Fred Tjallingii[1]*, Elisa Garzo[2] & Alberto Fereres[2]

[1]*Laboratory of Entomology, Wageningen University, PO Box 8031, 6700 EH, Wageningen, The Netherlands, and* [2]*Instituto de Ciencias Agrarias (ICA), Centro de Ciencias Medioambientales, Consejo Superior de Investigaciones Científicas (CSIC), C/ Serrano 115 dpdo, 28006, Madrid, Spain*

Accepted: 27 January 2010

Key words: full EPG, R-EPG, *Aphis gossypii,* Cucumovirus, Cucumber mosaic virus, CMV, non-persistent transmission, *Cucumis melo,* melon, *Brevicoryne brassicae, Myzus persicae,* Hemiptera, Aphididae

Abstract

Intracellular punctures by aphid stylets appear as potential drop (pd) waveforms in DC electrical penetration graph (EPG) recordings. We used a dual-EPG device that recorded in one channel the 'full EPG' with R-plus emf-components (i.e., the usual DC EPG) and concurrently in a second channel the 'R-EPG' with R-components only. The circuit of the latter channel was an optimised amplitude modulation (AM) version derived from early (before 1990) AC systems. We also made some 'emf-EPG' recordings using a separate high input resistance 'emf-amplifier' sensitive to emf-components only. The intracellular pd waveforms have previously been divided into three subphases, and we aimed to distinguish and separate these subphases more accurately by the dual-EPG recordings than with the normal full EPG only. In this study, we temporarily distinguished five subphases (α–ε), but unequivocal distinction of only a few of these appeared possible, in spite of the information coming from the two signals. The lack of clearly separable features in R-EPG signals often provided serious difficulties in pd recognition without the concurrent full EPG, but once located, only subphase II-2 features were clear and supported the II-2 data from the full EPG. Consequently, we could not distinguish subphases of complete pd waveforms better with additional R-EPG information during cell punctures by *Aphis gossypii* Glover (Hemiptera: Aphididae). In *Brevicoryne brassicae* (L.) (Hemiptera: Aphididae), however, distinguishing II-2 subphases in the full EPG was sometimes a problem. Our detailed dual-EPG observations showed some waveform continuity from halfway into the II-1 subphase (start of the newly recognised subphase β) until the end of the pd, with a strong but variable emf origin. This waveform tended to overrule other subphase waveforms in *B. brassicae* more than in *A. gossypii* and *Myzus persicae* (Sulzer) (Hemiptera: Aphididae). Subphase waveforms in full EPGs were especially difficult to recognise when pd periods had been interrupted in a virus inoculation experiment and additional R-EPG information could then be useful. This inoculation experiment showed again that only the first subphase (II-1) contributes to virus (Cucumber mosaic virus) inoculation by *A. gossypii*. In *B. brassicae*, the benefit of concurrent R-EPG information in such virus experiments is presently under further investigation. Apart from this special application to virus experiments, we do not recommend the routine use of the dual-EPG device. Furthermore, we do not advocate the distinction of more than the previously recognised three intracellular pd subphases as a feasible option in future studies. Analysis of EPGs with concurrent R-EPGs requires substantially more analysis work without yielding consistently useful additional insights. This confirms earlier dual-EPG results from thrips.

*Correspondence: W. Fred Tjallingii, Wageningen University, Laboratory of Entomology, PO Box 8031, 6700 EH, Wageningen, The Netherlands. E-mail: fred.tjall@epgsystems.eu

Introduction

Early intracellular punctures by aphid stylets are very effective in the transmission of non-persistent plant viruses

(Powell, 1991; Collar et al., 1997; Martin et al., 1997; Fereres & Collar, 2001). These cell punctures can be monitored electrically by using the electrical penetration graph (EPG) technique (Tjallingii, 1985b, 1988; Pettersson et al., 2007). Within 10 s after starting a probe (the period of stylet penetration), aphids are likely to initiate a cell puncture, which is reflected by a potential drop (pd) waveform in the EPG (Tjallingii, 1985a; Tjallingii & Esch, 1993). Many such punctures occur during the stylet pathway phase before the stylets reach the phloem sieve elements and the aphids actually start feeding. Potential drop waveforms show a sequence of three main phases, of which only the second phase (II) is intracellular; this has been divided into three subphases (II-1, II-2, and II-3). Using non-persistently transmitted plant viruses as markers, the first subphase has been linked to salivation and the third one to ingestion with respect to transmission of Cucumber mosaic virus (CMV) and Potato virus Y (PVY) (Martin et al., 1997; Fereres & Collar, 2001). This was inferred from experiments with interrupted cell punctures, in which efficient virus acquisition required occurrence of the third subphase (II-3), whereas occurrence of only the first subphase (II-1) was sufficient to allow efficient release of virus (inoculation) by viruliferous aphids. Furthermore, Powell (2005) used the persistent circulative Pea enation mosaic virus (PEMV) as a marker for intracellular delivery of saliva. He showed that aphids that had acquired PEMV as nymphs were able to inoculate this virus as adults during the first subphase of the pd. This work provides unequivocal evidence that intracellular salivation occurs during subphase II-1, because the circulative PEMV crosses the membranes of the accessory salivary glands (Gray & Gildow, 2003) and is then injected into the plant with watery saliva. Recently, localisation of the protein receptors of cauliflower mosaic virus (CaMV) in the common duct of the maxillary stylet tips (Uzest et al., 2007) suggests that salivation is the most likely mechanism involved in the inoculation of some semi-persistent viruses as well.

Harris & Harris (2001) assumed that the II-2 subphase (which they renamed as Kh-1b) represents egestion and suggested that this subphase is responsible for inoculation of non-persistently transmitted viruses. This assumption appears to be merely based on speculation, as no experimental evidence has been presented to support the claim that subphase II-2 is linked with the ejection of stylet contents and virus inoculation.

Development of the DC EPG recording system allowed recognition of pd waveforms and their relationship with intracellular punctures (Tjallingii, 1985b). The technique was subsequently instrumental in elucidating associations between intracellular subphases and virus inoculation and acquisition (Powell et al., 1995; Martin et al., 1997; Powell, 2005). Recognition of the pd waveform in the DC system was due to an electronic improvement (Tjallingii, 1988) of the original circuit of the 'electronic monitoring system' (EMS) introduced by McLean & Kinsey (1964). Later, the EMS was referred to as the 'AC system' (Walker, 2000). The main difference between the two systems is that in the EMS circuit (McLean & Weigt, 1968) an oscillator (alternating current, AC) voltage is applied to the plant whereas in the DC system this is a direct current (DC) voltage. The EMS device processed the amplitude of the AC voltage, which was modulated by the aphid's fluctuating electrical resistance during stylet penetration. The signal modulation and its later demodulation is known as amplitude modulation (AM) and the signal only contains components that originate as a result of changes in electrical resistance (R-components). Biologically, the resistance (or conductivity) fluctuations are thought to be caused by open or closed valves at the proximal end of the capillary stylet canals and by electrolyte concentration changes in plant sap and aphid saliva. In the DC system, the R-components directly contribute to the EPG (but need no signal processing) as the fluctuating resistance in the insect also modulates the DC voltage across the insect and plant (Walker, 2000). In addition, voltages that are generated during aphid–plant interactions simultaneously contribute to the DC EPG signal, and these voltages are referred to as electromotive force (emf) components. The emf-components also reflect important biological information, such as transmembrane potentials of punctured plant cells and streaming potentials caused by fluids flowing within the stylet canals (Tjallingii, 2000; Pettersson et al., 2007). No emf-components were recorded by the original EMS.

Recently, a completely modified EMS has been developed (Backus & Bennett, 2009). This so-called 'AC-DC correlation monitor' is a three-channel device to monitor one insect. The circuit of one channel is a copy of the DC EPG circuit, whereas the other two channels appear to be cumbersome, modified versions of the original AC signal processing circuit in which the AM design of the original EMS can be disabled (by a switch), thus losing an essential property of the former AC system design in these channels. The signals of these 'AC channels' with switched-off AM echoed the DC EPG signals, with only minor differences. Furthermore, when the AM processing was not disabled (reverse switch position), the authors could not record any EMS-like signal from these channels. It is therefore clear that this new 'AC system' does not refer any longer to a recorder of the R-component EPG (Walker, 2000). In this study, we will refer to signals from the DC system as the 'full EPG', recording components from both R and emf origin, and signals from the AM-optimised EMS circuit as the 'R-EPG', containing only R-components. Further-

more, we will use the term 'emf-EPG' to refer to signals from an amplifier with a high-resistance input, which records only the emf-components (Tjallingii, 1988). We thus relate the terminology to the essential property of the circuits and signals. If no separate R- or emf-EPGs are involved, future use of 'full EPG' will of course be redundant.

During discussions of the advantages and disadvantages of various EPG systems in the past, it has been suggested that recording full EPGs and R-EPGs (then called DC and AC EPGs) side by side could be interesting. The R-EPG signal is simpler than the full EPG because in the full EPG both electrical components are superimposed and interact in the recorded signal. This idea was proposed by Tjallingii (2000) and has been realised by constructing a dual-EPG system that concurrently records the full EPG and the R-EPG. The dual-EPG system was also used in a study with thrips and called the 'DC–AC EPG device' (Kindt et al., 2006), but comparison of its two signals did not allow better waveform recognition and separation than the full EPG signals only. Because of difficulties in recognising and separating subphases in full EPG cell punctures (pd waveforms), we made another attempt to achieve higher resolution using the dual system here, also stimulated by the importance of aphid signals in understanding virus transmission and its association with particular subphases as mentioned above. Based on earlier work (Reese et al., 2000), it appeared that the 'X waves' from an EMS system reflect R-EPG equivalent of the pd waveform from the DC system. Most X waves, however, were much less distinct when embedded in stylet pathway waveforms, as demonstrated by the fact that we discovered 'overlooked X waves' in the pathway signals published by Scheller & Shukle (1986), which were not recognised by the authors themselves.

Here, we first compared complete pd waveforms in full and R-EPGs by using the dual system to record from *Aphis gossypii* Glover, *Brevicoryne brassicae* (L.), and (less extensively) *Myzus persicae* (Sulzer) (all Hemiptera: Aphididae). Subsequently, we applied the dual-EPG system and the results of this analysis in a CMV inoculation experiment with interrupted pd waveforms, in order to test whether a possibly improved separation of subphases would provide clearer results than those obtained in the past using full EPG signals only.

Materials and methods

Aphids and plants

Aphids were reared in a growth chamber at L16(23 °C):D8(18 °C) photoperiod and 60 ± 10% r.h. *Aphis gossypii* was reared on melon, *Cucumis melo* L. cv. 'Primal' (Cucurbitaceae). *Brevicoryne brassicae* and *M. persicae* colonies were reared on turnip, *Brassica rapa* L. cv. 'Just Right' (Brassicaceae). Melon and turnip test plants used for EPG recoding and CMV transmission tests (melon only) were sown in 5 × 5 cm plastic pots and kept in a growth chamber at L16(26 °C):D8(20 °C) photoperiod and 60 ± 10% r.h. Melon seedlings were inoculated with a CMV isolate kindly supplied by Dr. E. Moriones; it was originally obtained from melon in Valencia (Spain) and maintained in desiccated tissue at 4 °C. Cucumber mosaic virus was mechanically inoculated to melon plants (cv. 'Primal') using 0.03 M Na_2HPO_4 and 0.2% diethyl dithiocarbamic acid plus carborundum. Newly CMV-infected melon source plants were generated by aphid inoculation 2 weeks before experiments began.

Virus inoculation experiments

Apterous adult virginoparae of *A. gossypii* were collected from the colony and wired about 1 h before the experiments started. Wiring was done by fixing the aphid on a vacuum needle (van Helden & Tjallingii, 2000), applying a small droplet of water-based silver glue (EPG Systems, Wageningen, The Netherlands) to attach a 1- to 2-cm gold wire, 20 μm in diameter. The other end of the gold wire had been previously attached with silver glue to a thin (0.2 mm) copper wire of about 2 cm, which was soldered onto a brass pin, together forming the insect electrode. Wired individual aphids were connected to the first-stage amplifier (Figure 1) and a 10-cm long, 2-mm thick (copper) plant electrode was inserted into the soil. To increase virus acquisition efficiency and to obtain recordings of complete pd waveforms, we first monitored the aphid probing a potted CMV-infected melon source plant. The aphid was allowed to perform one first complete pd waveform within a probe, which was displayed and observed on the computer monitor. The aphid was lifted off the plant immediately after this CMV acquisition puncture, and the source plant removed and replaced by the first healthy test plant for monitored inoculation access. The melon (cv. Piel de sapo Ricamiel) test plants were seedlings with one or two true leaves. The plant electrode was inserted into the soil of this test plant and the same wired aphid was now allowed to initiate an inoculation probe. During the intracellular phase (II) of the first pd, the aphid was lifted while attached to the first-stage amplifier, thus interrupting the inoculation puncture. The subphase(s) performed before the interruptions were established later, when waveforms were analysed. Aphids that were allowed to complete an inoculation puncture were lifted after stylet withdrawal from the cell. Subsequently, the gold wire was cut close to the aphid dorsum with fine scissors, and the aphid was transferred to a second test plant seedling that

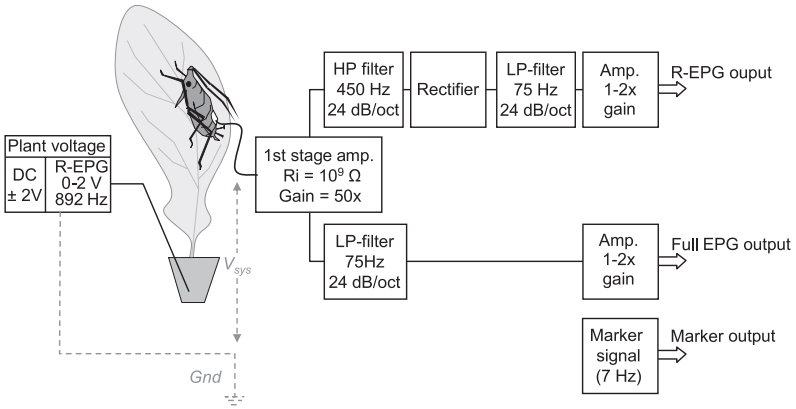

Figure 1 Recording system with two output signals from the dual-EPG amplifier and one from a marker device, which is used in the virus transmission experiment only. The plant voltage is the sum of voltages applied to the plant: (1) the usual DC voltage, (2) the AC oscillator voltage. The AC voltage (maximally 2 V peak–peak) was adjusted at 0.5 V constantly, but the DC voltage was adjusted to a voltage according to what was needed for each individual insect. This voltage is added up to the two unpredictable electrode potentials (at the soil and aphid electrode interfaces) to achieve a final voltage across plant and insect (V_{sys}) and its adjustment is controlled on bases of the full EPG output signal. After the usual first-stage amplifier (1 GΩ input) the signal is split into a full EPG branch, in which the signal passes an LP filter (cut off frequency at 75 Hz; dB/oct = steepness of filter) and an R-EPG branch filtering out the DC voltage and low-frequency signals by a high-epass filter (cut off at 450 Hz). Then, the R-EPG signal is processed further by a rectifier and a smoothening LP filter (cut off at 75 Hz). Both signals can be amplified finally up to twofold. The marker device is used to record 7 Hz signals to mark the start of virus acquisition and inoculation sessions in a separate concurrently recorded signal.

was covered by a transparent inverted plastic cup for about 24 h. Cups and aphids were removed then and second test plants were sprayed with Confidor® 20LS (imidacloprid, 20%; Bayer, Monheim, Germany) to kill any overlooked aphids and offspring. This second test plant was used to assess the initial virus acquisition success; aphids that had not infected either of the two test plants were omitted from data analysis.

EPG recording

The dual-mode EPG amplifier (Tjallingii, 2000) was the same one used by Kindt et al. (2006), which was there called the DC–AC EPG system. The full-EPG channel in this amplifier is essentially identical to the usual DC EPG amplifier (Tjallingii, 1985a, 1988), except for a low pass (LP) filter, used to strip the superimposed oscillator frequency and its modulations now additionally introduced into the aphid–plant circuit (Figure 1). For the R-EPG, the oscillator (AC) voltage at a frequency of 892 Hz and 0.5 V peak–peak amplitude was added (by a summator circuit; not shown) to the adjustable DC plant voltage and supplied to the plant electrode (Figure 1). The system voltage (V_{sys}) indicated in Figure 1 is the actual DC voltage across the aphid–plant combination and is the sum of the (unpredictable and drifting) electrode potentials and the DC voltage supply from the plant voltage unit. The first-stage amplifier was not modified and had its usual 1 GΩ input resistor and 50 × gain. Then, the signal was split into two branches, with one channel for the full EPG with the LP filter (fc = 75 Hz; 24 dB/oct) and the R-EPG channel with high pass filter (HP, fc = 450 Hz; 24 dB/oct) stripping all low frequencies of the usual DC signals and allowing only oscillator frequency and its modulated amplitude to pass to the further AM signal processing circuit. This included a single-phase rectifier (which, at 892 Hz frequency, did not affect the signal quality) and a LP filter (fc = 75 Hz; 24 dB/oct) smoothing any oscillator frequency remnants. The R-EPG branch in our dual-EPG amplifier was in fact an AM optimised version of the design in EMS and other AC systems dating before 1990 (Tjallingii, 2000; Walker, 2000), which recorded only the R-components in the EPG. In both branches, a final one to two times extra output gain allowed an adjustable total gain between 50 and 100 × (Figure 1).

For EPG recordings, a Faraday cage was used containing only the plant, the aphid, and the first-stage amplifier. The other parts (Figure 1) were housed in a 'control box' and were located outside the cage, with the AD converter (DATAQ Di710 [14 bit] or Di158U [12 bit]; USB). Data acquisition of two EPG signals and an additional marker signal (see below) were digitised at 100 Hz sampling, mediated by PROBE 3.0 software (originally Wageningen University, now distributed by EPG Systems) displaying these three signals during recording. In the marker signal,

pushbutton operated brief signals of 7 Hz (±5 V) were generated by a separate device (Wageningen University). The signals marked the start of a new acquisition or inoculation session for each aphid within the continuous 1-h recordings.

In order to compare the dual-EPG signals on the one hand, with signals containing only emf components on the other, some pure emf recordings (*B. brassicae* on turnip only) were made by a high-input resistance (150 TΩ) amplifier (Tjallingii, 1985a). The emf-EPG cannot be recorded simultaneously with full or R-EPGs (Tjallingii, 2000).

Signal analysis

Signals were analysed using a slightly modified version of PROBE analysis software (EPG Systems) to estimate the starting times of all newly distinguished waveform details. First, we estimated these in all full EPG recordings and subsequently this was done in all R-EPG recordings. The full EPG starting times of the pd waveforms were used to help locate pd periods in the R-EPG, as it was difficult to find them without such indications. However, full and R-EPG signals were not simultaneously displayed on the same analysis screen, and no information from the full EPGs was used for subsequent R-EPG subphase distinction. In total, 59 first pd waveforms in the CMV acquisition probes were used to compare starting times from full and R-EPG signals by *A. gossypii* on melon and 57 first pd waveforms in probes by *B. brassicae* on turnip. The time difference obtained by subtraction of the established R-EPG starting times from full EPG starting times in each pd signal pair was used to express synchrony between full EPG and R-EPG per subphase. In each interrupted pd waveform from the CMV inoculation experiment, we scored the subphases occurring. Pairwise comparisons between the transmission rate after the different waveform subphases were analysed using a χ^2-test and by Fisher's exact test when expected values were lower than 5. Analysis was done using Statview 4.0 software for MacIntosh (Abacus Concepts, Berkeley, CA, USA).

Results and discussion

General features of pd waveforms in the full and R-EPG

Three main waveform phases that have previously been distinguished in pd signals of the DC system (referred to as full EPG waveforms here) are the main phases I, II, and III, of which only phase II is intracellular. Within phase II, three subphases, II-1, II-2, and II-3, have been defined so far (Tjallingii, 1985b; Powell et al., 1995). Most complete pd waveforms that were recorded here showed these subphases during probes by *A. gossypii* and *M. persicae* on melon and *B. brassicae* on turnip. The subphase waveforms identified were very similar to those described earlier (Powell et al., 1995; Collar et al., 1997; Martin et al., 1997; Powell, 2005). Nonetheless, a closer look at details suggested that a finer discrimination into more subphases might be desirable, at least for this study. Therefore, we decided to temporarily distinguish five new subphases within phase II, indicated as subphases α–ε (Figure 2).

Estimation of the beginning and end time of each pd main phase II (intracellular pd period) and the new subphases α–ε was not always possible as not all subphases could be distinguished in each pd waveform (Figure 3). Subphases β and ε (Figure 3) were particularly problematic. In *A. gossypii* recordings, subphase β could not be distinguished in about 50% of the full and R-EPG traces; in about 70% of the full/R-EPG pairs, no subphase β could be distinguished in one of its traces. In *B. brassicae*, subphase β was much clearer in the full EPG (93%, Figure 3; Figure 2B, top trace) but in the R-EPG it was the opposite; β was clear in only 5% of cases (Figure 3). Similarly, subphase ε could not be distinguished or did not occur in more pd waveforms than subphases α, γ, and δ (Figure 3). The starting time 'synchrony' between the full and R-EPG main- and subphases is given in Figure 4; the shortest bars reflect the best synchrony and a positive value indicates a later start in the full EPG. Subphases β and ε showed the poorest synchrony.

The main phase II in the full EPG shows two clear edges (voltage shifts), one at the start and one at end of this main phase, respectively (Figure 2, full EPG traces). The first edge from main phase I to II shows a negative voltage shift reflecting stylet insertion into a cell and through the plasmalemma, and the second edge from main phase II to III shows a positive voltage shift reflecting stylet withdrawal from the cell membrane. The sustained negative voltage indicates an intracellular stylet tip position in the intact cell. The transmembrane potential is an emf–component and consequently, the R-EPG traces do not show the edges. The R-EPG equivalent of the pd (originally indicated as the 'X-wave'; see McLean & Kinsey, 1964; Reese et al., 2000) starts as a low-flat period – reflecting a decreased electrical conductivity, possibly due to 'sealing' of the stylet tip by the plasmalemma just before the puncture – mostly starting before and ending after the steep first edge of the pd in the full EPG trace. A similar low-flat period in the R-EPG occurs at the transition between phases II and III of the full EPG pd (Figure 2; 'LF' in bottom traces).

Although the leading edge of the pd (phase I–II transition) was clear in most full EPG traces, sometimes it was not. In *A. gossypii*, 28% of the first pd waveform in probes we studied showed no steep edge, but a gradual change from extra- to intra-cellular potential instead (Figure 5A).

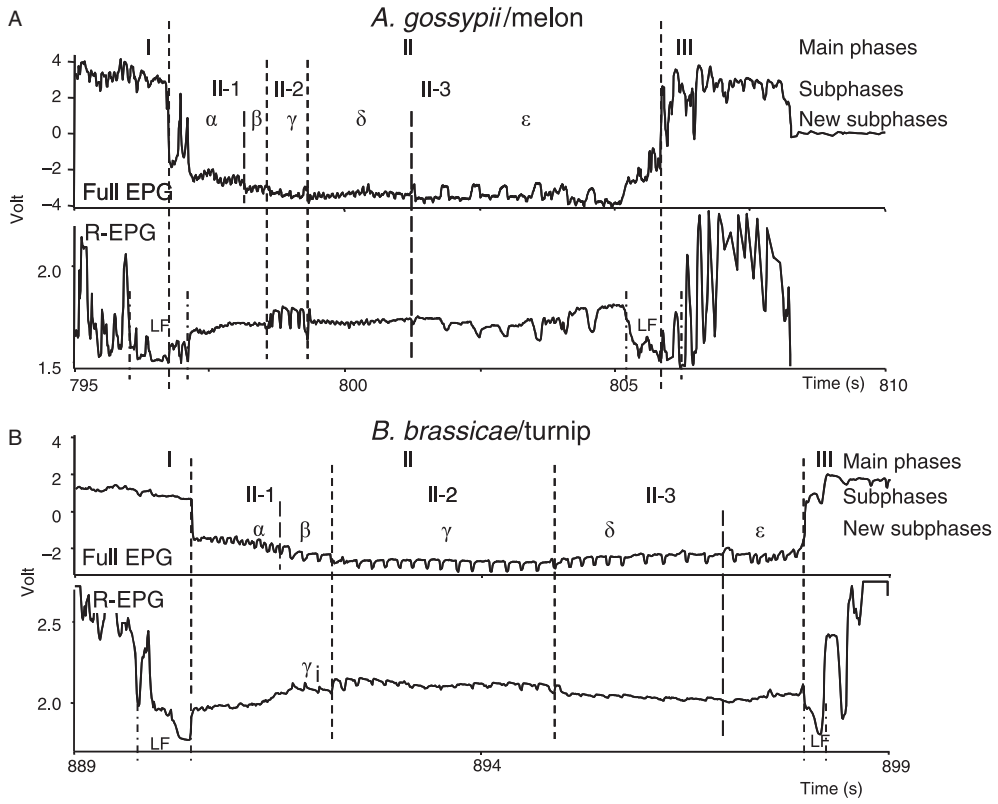

Figure 2 Two pairs of concurrently recorded full and R-EPGs of complete pd waveforms reflecting intracellular stylet punctures from (A) *Aphis gossypii* and (B) *Brevicoryne brassicae*. Three main waveform phases (I, II, and III) have been distinguished but only phase II represents the intracellular part in which the three subphases, II-1, II-2, and II-3 occur. Here, we temporarily distinguish five new subphases of which the full and R-EPG properties are described and compared. The γ_i initial part of subphase γ appeared in R-EPG signals, almost exclusively. Dashed vertical lines show the subphase borders as established after identification and description of waveform features, but no such line is drawn for subphase β in the R-EPG of both aphids as in these recordings no α–β transition could be distinguished. In Figure 8, they could, in contrast. LF indicates the low-flat R-EPG periods between dash-dot lines; subphase ε is hardly distinguishable as such here (one low pulse only at the dashed line for ε). Note the similarity between β, γ and δ features in full EPG recordings of *B. brassicae*.

The high amplitudes of waveforms A and B (Tjallingii, 1988) apparently interfered and masked these starting edges. Also, even more pd waveforms (39%) started with more than one edge, presumably reflecting a number of successive, brief membrane punctures and withdrawals either preceding or performed during the first subphase α activities (Figure 5B). This made it difficult to decide which edge to consider as the start of the pd period and subphase α. Similar difficulties were encountered with *M. persicae* and (less frequently) with *B. brassicae*. It seemed that in the beginning of the gradual slope or at the first of the multiple pd edges, the subphase α features (see below) had started already. The relatively small amplitudes of subphase α then seemed to continue superimposed on the high-amplitude waveforms although were often difficult to distinguish as such. In our measurements, we always took the first recognisable feature of subphase α and the first of two or more edges as the starting time.

The pd features in the R-EPG were much less clear and – as described previously – we located pd periods in R-EPGs on the basis of pd features in the corresponding full EPG signals. Gradually starting pd waveforms or multiple edges in the full EPG signals showed no or hardly any features in the R-EPG counterpart signals so that the R-EPG could not be used to clarify uncertain full EPG features. Taking the first edge (phase I) as the pd start in the full EPG and the beginning of the low-flat period as the start in the R-EPG pd, the full/R-EPG synchrony was poor – as reflected by the long and positive bar (Figure 4; pd^{st}) – with the full EPG starting after the R-EPG start. However, when we took the end of the low-flat period as the start of the pd period in the R-EPG, subphase α in fact, it started consistently later than subphase α recorded by the full EPG (negative bar; Figure 4). Although the full/R-EPG synchrony of subphase α was rather good (close to zero) in both aphids, in *B. brassicae* it was opposite (Mann–Whit-

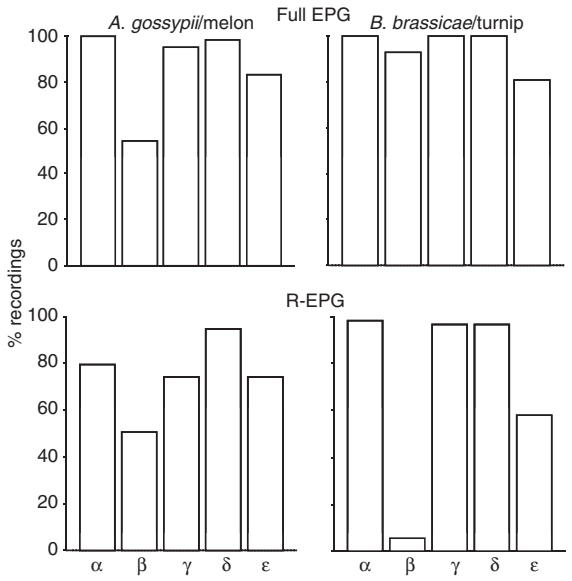

Figure 3 Subphases that could be distinguished in the full EPG and concurrent R-EPG recordings in two aphid species, *Aphis gossypii* and *Brevicoryne brassicae*. Bars represent the percentage of recordings in which the start of each of the subphases could be distinguished. If the next bar is shorter than the previous (from left to right), this shortfall represents the proportion of recordings in which no start of that subphase could be established and thus, no distinction could be made between the subphases. Possibly, the underlying subphase activities might have occurred, but the associated waveforms were too weak to become visible.

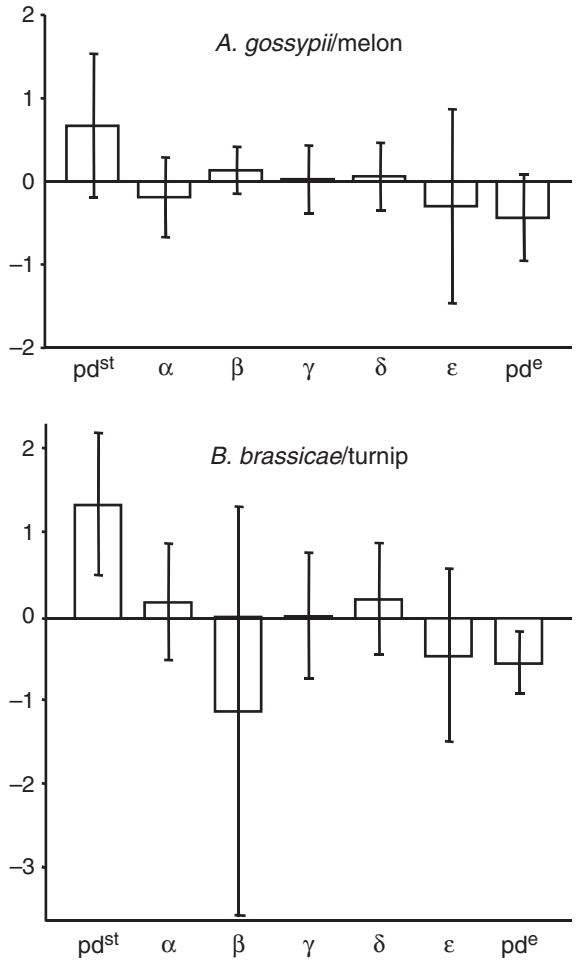

Figure 4 Synchrony of starting times of full and R-EPG subphases expressed as the mean difference (± SEM) between full and R-EPG starting times. High correspondence means a small difference (short bar) and positive bars reflect a later full EPG start, negative bars an earlier full EPG start than the respective R-EPG subphase. pd^{st}, synchrony of start of pd period based on start of first low-flat period in R-EPG as compared to start of subphase α in full EPG; pd^{e}, synchrony of end of second low-flat period in R-EPG as compared to end of subphase δ(+ε) in full EPG (see Figure 2).

ney U-test: $P<0.01$; positive bar; Figure 4), which may be due to differences between the two species with respect to timing of activities but more likely, due to differences in reflection of activities in EPG signals (see below). Most of the low-flat period seems to correspond to what has been considered earlier as the extracellular part of main phase I in full EPGs (Figure 2; Tjallingii, 1985b). The end of the main phase II, i.e., the end of subphase ε, was also much less clear in R-EPG than in full EPG traces. The R-EPG low-flat period did not end consistently later than the full EPG withdrawal edge (Mann–Whitney U-test: $P = 0.18$; negative bar; pd^{e} in Figure 4). This suggests that although the period of increased resistance extends for longer than the intracellular stylet tip position, this may often be masked by subsequent signal elements. Also here, the R-EPG low-flat that extends beyond the full EPG edge might be considered as main phase III. However, so far neither the full EPG main phase I nor III have been studied in detail or defined. Only 'some differences' with the other pathway waveforms have been mentioned (Tjallingii, 1986).

The large variation in waveform shapes during subphases in the recorded full EPGs are to be expected. It is an intrinsic property of the DC system that across every insect there is a different DC system voltage (Figure 1, V_{sys}). This voltage is caused by electrode potentials (from plant and insect electrodes) in addition to the manually controlled plant voltage supply. The supplied plant voltage is adjusted at the beginning of each new recording to an optimal output level (the highest amplitude of pathway waveforms). However, there is always a slow drift of the electrode potentials over the course of time and as it is not wise to adjust the plant voltage frequently the recorded output level (y-axis value) often

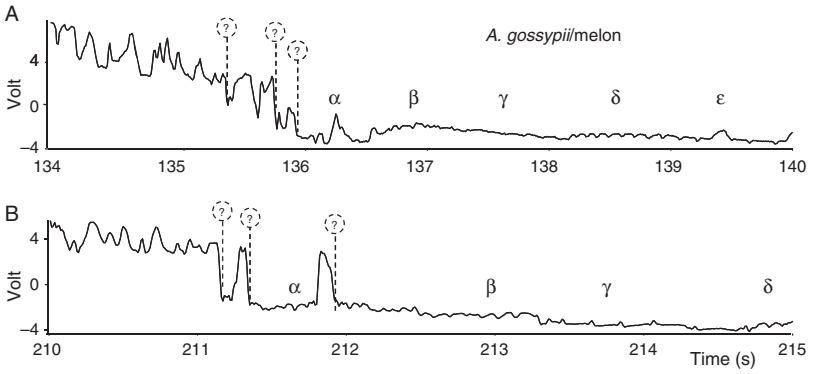

Figure 5 Two unclear beginnings of full EPG subphase α. (A) Gradual slope instead of steep edge due to interferences with high amplitudes of pathway waveforms (A and B) during the early probe make it difficult to decide when it starts. (B) Multiple edges presumably due to successive cell membrane penetrations during the beginning of the pd period. Which edge marks the beginning of subphase α (the pd main phase II) is unclear. The ?-marked dashed lines all indicate a possible start. In both cases, the first features of subphase α and the first edge, respectively, were chosen as the starting time.

becomes lower or even negative (Tjallingii, 1985a, 1988, 2000), which affects the R-component in the full EPG. Consequently, with a lower plant voltage the R-/emf-components ratio becomes smaller, and with a negative system voltage, the R-EPG signals become inverted. This makes the R-/*emf-component interactions complicated and will contribute to the variability of the full EPG signals. In the R-EPG circuit, this system voltage (DC) plays no role because only the constant voltage (amplitude) of the oscillator is important. The magnitude of the R-components in the R-EPG is not affected by plant voltage differences between recordings. Nevertheless, between pd periods in R-EPGs considerable differences were observed (cf., R-EPG traces of Figures 2A and 6A) thus demonstrating a considerable variability within R-components. Also, among pd periods of emf-EPG signals – as recorded by the emf-amplifier – considerable differences occurred (Figure 7). Thus contributions of both components can differ between pd periods as well as between subphases within a pd period. Because these differences cannot be fully explained by system voltage differences, the variability of subphase waveforms is most likely due to natural variation in the aphid's activities, such as intensity and timing of the underlying mechanics.

Individual subphases

Subphase α. The full EPG features of subphase α showed a sine wave-like shape (Figure 6) at a frequency between 10 and 15 Hz (rectangle frames), although the regularity was often masked (especially at the start) by interference from slower and faster waveforms, making its frequency difficult to determine (Figures 2A and 6B; full EPG traces). Such irregularities during subphase α generally decreased in the later part of the subphase. In contrast, in most R-EPG recordings subphase α showed hardly any details (Figures 2 and 6; R-EPG traces), indicating that this waveform is almost completely of emf origin. However, the R-EPG trace occasionally showed a similar signal as the full EPG trace, thus demonstrating that a concurrent R-component can be involved sometimes. As part of subphase II-1, the activity recorded as subphase α has been related to watery salivation (Martin et al., 1997; Powell, 2005) and the sine waves might be caused by fluctuations in saliva flow inside the salivary stylet canal as caused by the salivary pump.

Subphase β. Subphase β – the second part of the II-1 subphase – has been distinguished mainly on the basis of full EPG waveform features, which deviate from the preceding sine waves in subphase α. The wave tops become flattened and increase in duration, resulting in a frequency decrease to 8–10 Hz (Figures 2 and 5). The flat tops of subphase β sometimes showed a small negative deflection half way (cf. full EPG trace in Figure 8A), and the transition to subphase γ was sometimes gradual. Especially in *B. brassicae*, features in most β subphases often differed more from subphase α than from subphase γ (Figure 2B and 6B). The R-EPG subphase β has no clear waveform features, which is similar to subphase α, and therefore, any full/R-EPG feature relations are lacking. In the R-EPGs by *A. gossypii*, subphase β could be distinguished by a sudden voltage increase, in about half of the recordings but in *B. brassicae* in only about 5% of the R-EPGs (Figure 3). This sudden increase in the R-EPG occurred when subphase β in the full EPG started (Figures 6 and 8A).

Subphase γ. The initial part of subphase γ is shown earlier in many R-EPGs than in the full EPG, which is still show-

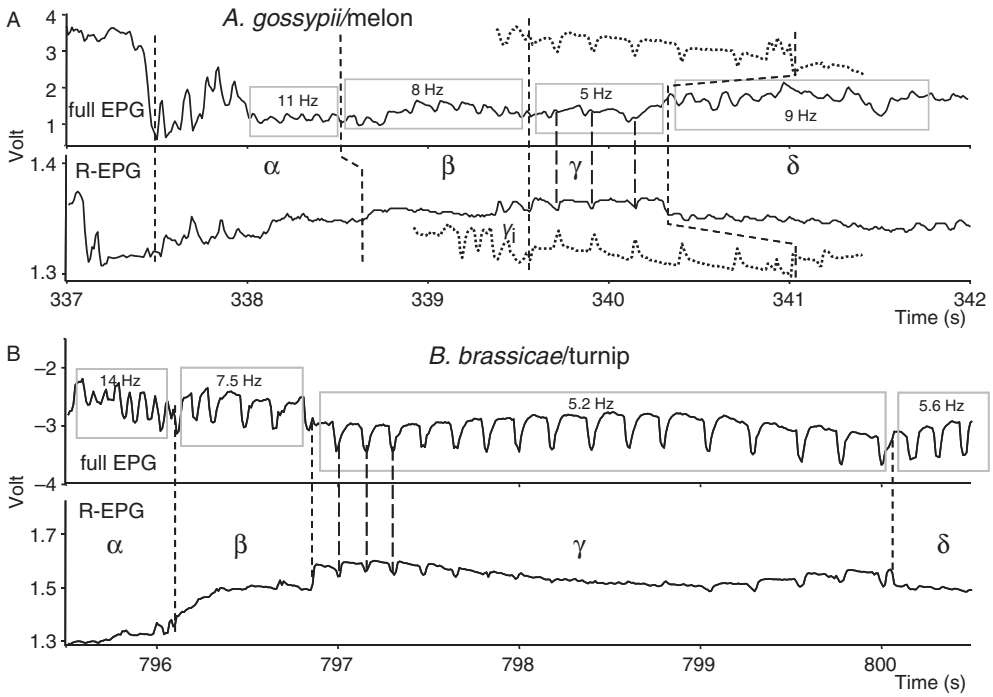

Figure 6 Two pairs of more detailed full and R-EPG counterpart signals with pd (separated by lines with short dashes) up to subphase δ only (5 s). Mean frequencies of subphase waveforms are shown inside rectangles (full EPG). R-EPG traces show clear features only during subphase γ and the preceding γ_i. Vertical lines with long dashes indicate full/R-EPG synchrony of spikes within subphase γ (beginning only). (A) *Aphis gossypii*, with full EPG subphase γ features distinctly different from subphases β and δ. Dotted traces show a typical feature divergence of subphase γ in this aphid (see text). (B) *Brevicoryne brassicae*, showing only small differences between subphase β, γ, and δ. R-EPG subphase γ features with reduced downward spikes during the middle part may occur.

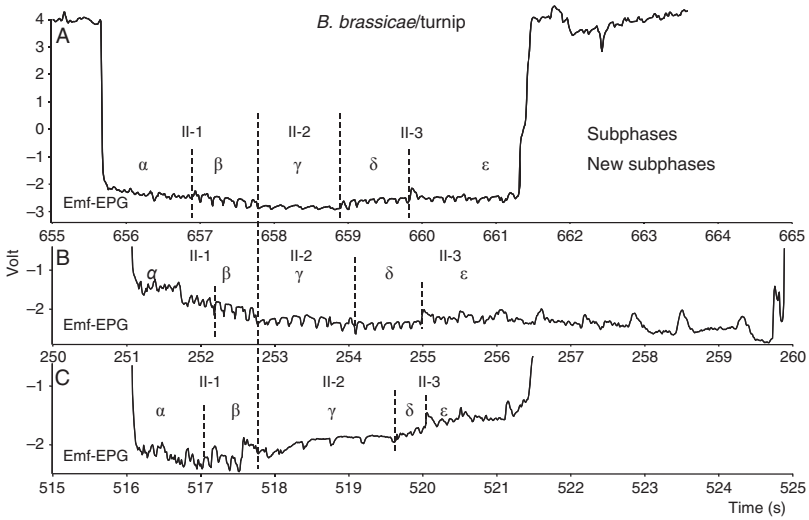

Figure 7 Examples of 'pure emf-components' in three separate pd periods, as recorded by the emf-amplifier from *Brevicoryne brassicae* on turnip. The full EPG waveforms illustrated in Figures 2 and 6 are in fact the result of the emf-components as shown here, added to the 'pure R-components' as shown in the R-EPG traces. (A) Continuous waveform features from subphase β to the end of δ with a reduced amplitude during subphase γ. (B) As A but with higher γ amplitude; ε pulse amplitudes also increasing and more numerous in long pd (with long δ + ε). (C) 'Repetitive pd' waveform with very much reduced frequency during subphase γ.

ing subphase β then. This part of subphase γ showed one or more separate waves or spikes, going positive with respect to the previous voltage level. Subsequently, the second or principal part of subphase γ was shown starting and ending with the subphase γ features in the full EPG. The R-EPG γ subphase showed a plateau maintained at the voltage level of wave tops of the initial γ part. This plateau is interrupted regularly by brief downward spikes

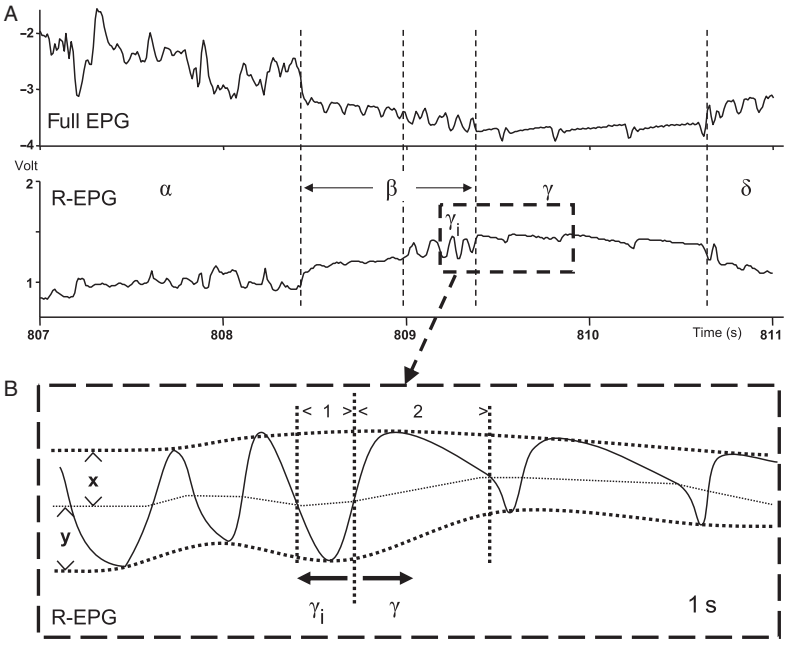

Figure 8 Clear γ_i initiation of subphase γ in pd period of R-EPG. (A) Waveform pd from *Aphis gossypii* on melon with γ_i preceding subphase γ in R-EPG trace. The full EPG trace also reflects some changes (disturbances of the β waves) during subphase γ_i in the R-EPG. (B) Criterion for the transition from γ_i to γ in the R-EPG signal (abstracted from dashed area in A). Subphase γ was defined as starting when a positive wave phase <2> has a two times or longer duration than the preceding negatively going wave phase <1> when measured halfway between a wave maximum/minimum and its subsequent minimum/maximum, respectively, i.e., when x equals y.

(sometimes shown as a saw tooth) at a much lower frequency than the initial, separate waves or spikes (Figures 2, 6, and 8A; R-EPG traces). In some longer lasting subphase γ periods, the plateau level as well as the downward spikes decreased somewhat in the middle (Figure 6B). In 34% of the recorded *A. gossypii* pd periods, no first part with the separate waves or spikes was shown, which is similar to the recordings from the other two aphid species. In fact, the number of separate waves recorded at the start of γ using the R-EPG varied from zero (34% of pd periods in *A. gossypii*) to about 4, maximally. If the separate waves or spikes occurred, the full EPG traces still showed the subphase β features, although sometimes interference could then be observed (Figure 8A). This means that the first part of the γ subphase overlaps with the β subphase whereas the principal subphase γ in the full and R-EPG always coincided. We decided, somewhat arbitrarily, to consider the initial part of subphase γ as an introduction rather than the real start of γ as such or a separate subphase and therefore, we labelled it γ_i. If γ_i occurred, it always started distinctly later than subphase β, thus suggesting no direct relationship between γ_i and β activities. Further, the interference observed during β in some full EPGs during γ_i suggests two overlapping underlying origins rather than one.

The principal γ subphase waveforms (spike or saw tooth features) showed a repetition rate (frequency) of 2–7 Hz (mean = 4.7 Hz in *A. gossypii* and similar in *B. brassicae*), which is distinctly lower than the frequencies in the preceding subphases α and β. Initially, the frequency can be similar to subphase β but decreases then during γ, either gradually (Figure 6A) or more abruptly (Figure 8A). During long recordings (not the regular short recordings used here for signal analysis), *B. brassicae* showed some later pd waveforms with 'repetitive pd' features (Tjallingii & Gabrys, 1999), that had a much lower frequency (Figure 7C; 0.5–1.8 Hz). However, such repetitive pd features in subphase γ were not recorded in the first pd periods in probes and not at all in pd periods of *A. gossypii* and *M. persicae*.

The shape of the full EPG subphase γ waveform showed a lot of variation within and between species. In the majority of *B. brassicae* recordings, the subphase γ waves showed the same flattened wave tops regularly alternating with negative spikes as in subphases β (Figures 2B and 6B), and also continuing in subphase δ (see Subphase δ section). The β-γ transition was inconspicuous, only showing a small change in frequency or voltage level at the beginning of subphase γ. In contrast, the majority of *A. gossypii* (and *M. persicae*; no signals shown) recordings showed positive spikes (Figures 5B and 6A, dotted trace) or bi-phasic spikes (Figures 2A, 6A, and 8A) rather different from the subphase β features and a much clearer β–γ transition. The β–γ similarity was initially apparent in *B. brassicae*, but later we realised that it occurred in few pd waveforms with *A. gossypii* as well, and the other way around, few pd waveforms in *B. brassicae* showed clear β–γ transitions. Thus, although the differences between the species were obvious in general, they were not consistent.

Consequently, during recordings with high β–γ similarity, interrupting the pd episode just before subphase γ would risk misinterpreting the β features as subphase γ in the full EPG. Therefore, the R-EPG features might be helpful in estimating the last subphase in such interrupted pd periods when using *B. brassicae* in virus experiments. In our *A. gossypii*/CMV inoculation experiment, this was less relevant as in this aphid the β–γ similarity is less common.

The R-EPG features of subphase γ_i and γ are in fact the only distinct aspects during the pd periods in these recordings. As stated, the subphase γ starts by a shift to a higher voltage level with regular negatively directed spikes. The R-EPG spike shape (not the amplitude) showed considerably less variation (among recordings) than full EPG spikes of subphase γ (Figures 2, 6, and 8) although within the R-EPGs of *A. gossypii* there seems to be a divergence between two types of subphase γ features. In about 10% of the analysed pd periods, the subphase γ signal was inverted, i.e., a shift to a more negative voltage level at the start followed by positively directed spikes (Figure 6A, dotted trace in R-EPG). In these cases, the features in the full EPG subphase γ of *A. gossypii* became similar to *B. brassicae* (compare dotted trace above full EPG in Figure 6A with full EPG in Figure 6B). It remains unclear what the cause of these two types is. They can be shown by the same *A. gossypii* individual and there is no relationship to the level of the voltage output. The same subphase γ divergence was shown by *M. persicae*, but not by *B. brassicae*. In spite of its clear R-EPG features, γ subphases could not be distinguished in about 25% of the recorded pd periods of *A. gossypii* but in *B. brassicae* they were clear in nearly all of the recorded pd periods (Figure 3).

Comparing pd periods in a sample of full and R-EPGs allowed development of an objective criterion for the transition point between γ_i and γ (Figure 8B). In accordance to this, we estimated the starting times of subphase γ in all full and R-EPG recordings. The resulting full/R-EPG synchrony for the start of subphase γ appeared to be the best synchrony of all subphase (Figure 4; shortest bar). The end of subphase γ (i.e., start of subphase δ) also showed very good synchrony, thus indicating that the subphase γ could mostly be derived well from full and rather well from R-EPGs (Figure 3), although in *A. gossypii* the R-EPG start of subphase γ was the least clear.

We also looked at the full/R-EPG synchrony of waveform features within subphase γ. In *B. brassicae*, the downward negative spikes shown during the flat plateau in R-EPG signals coincided with negative spikes in the full EPG counterpart signals (Figure 6B). However in *A. gossypii*, the negative R-EPG spikes coincided with the positive phase just after the negative in the biphasic full EPG waves separating the flat periods (three of them are indicated in Figure 6A by dashed connecting lines).

The clear R-EPG features reflect a strong R-component in the subphase γ signal, but apparently an emf-component is superimposed as shown by the full EPG traces and the separate emf recordings (Figures 6A and 7). In most full EPG signals by *B. brassicae*, the emf-component of subphase γ seems to overrule the R-component, whereas in *A. gossypii* (and *M. persicae*) this emf-component seems less strong as appears from the larger variation within full EPG signals. Thus, R-component and emf-components vary in strength substantially.

No correlation for subphase γ (previously designated subphase II-2) has been established to any aphid activity so far, although it has always been recognised as a clear landmark in the pd waveform. Our results confirm the clear signal features but do not reveal any waveform correlation. What makes subphase γ_i and γ rather special is their distinct R-EPG features, in contrast to rather weak R-EPG waveform features of the other subphases. This suggests that the two voltage levels between which the positive and negative spikes are alternating might represent the open (high voltage) and closed (low voltage) position of a valve associated with one of the stylet canals, possibly the cibarial valve or the (anatomically less clear) salivary duct valve. If so, the γ_i signal may suggest that some brief open valve periods (separate waves or spikes) precede a constantly open position during the main subphase γ with weak closing movements at low frequency. Additionally, the emf-components may be due to flow pulses (streaming potentials) of plant sap or saliva (or both) in the stylet canals driven by passive (cell turgor) or active forces by the cibarial and/or salivary pump. This is mere speculation, but we will come back to this point in the virus transmission section of this article.

Subphase δ. The features of subphase δ in the full EPGs from *A. gossypii* mostly showed a distinct change from the preceding γ features. A sine wave-like waveform was shown at a frequency of about 8–12 Hz, gradually decreasing to 4 Hz or less while its shape changed to flat topped long waves separated by sharp negative spikes, similar to subphase β. In *B. brassicae*, the change was distinct in spite of the more or less continual similarity of subphase features from the start of β until the end of ε. In contrast, hardly any detail could be distinguished in the R-EPG, although some R-EPG recordings showed very weak sine waves similar to the full EPG signal (Figures 2 and 6). This indicates that the δ features are predominantly of emf origin.

As subphase γ has clear R-EPG features, the start of subphase δ was clear and characterised by a shift to a lower

voltage level (R increase; Figure 3). Subphase δ was found to start slightly later in the full than in R-EPG traces, with the delay more marked in *B. brassicae* than in *A. gossypii* (Figure 4). Biologically, subphase δ likely reflects sap ingestion due to its experimental correlation with non-persistent virus acquisition (Powell et al., 1995; Martin et al., 1997).

Subphase ε. Subphase ε has been defined here as starting with the first of its typical and always positive pulses in the full EPG (Figure 2A for *A. gossypii*; Figure 7B for *B. brassicae*). Although the later pulses are mostly clear, the first pulse is often inconspicuous, especially in the R-EPG, in which all ε pulses are mostly weak and negative, opposite to the full EPG ε pulses. The full EPG pulse is flat topped and generally, starts and ends somewhat earlier than the negative R-EPG equivalent. As full EPG pulses remain positive regardless of the system voltage polarity, their major origin is emf and this apparently always overrules the weaker R-component shown in the R-EPG (Figure 2B is more representative than Figure 2A here; 2B also shows only one ε pulse at the left dashed line of ε). Due to the unclear first pulses in both of the traces, the starting time synchrony of subphase ε showed a large variation and was mostly detected one or two pulses later in the R-EPG signal, resulting in a high negative full/R-EPG difference (Figure 4). Pulses occurred at a frequency of 1–3 (mean = 1.4) and 1–2 (mean = 1.5) per pd period in *A. gossypii* and *B. brassicae*, respectively. However, up to 26 pulses have been observed in one long pd period (22.5 s), the δ + ε period especially (19.2 s). In 15% of the pd waveforms in *A. gossypii* and 11% in *B. brassicae* – especially the shorter ones – no ε pulses at all occurred and therefore, no subphase ε could be distinguished. After the ε pulses had started, the subphase δ features were continuing unchanged, indicating that as a matter of fact, there is no reason to distinguish a separate subphase ε as such.

Chen et al. (1997) divided pd waveforms produced by *A. gossypii* into standard (pd-S) and long pd (pd-L) waveforms, the latter having more than three pulses and occurring mostly as the first pd in a probe. When we divided our first pd waveforms into pd-S and pd-L groups according to the same criteria, we found some graphical support for a bimodal distribution indeed, although less in *B. brassicae* than in *A. gossypii*. The mean duration of subphase δ(+ε) was longer in *A. gossypii* (11.89 s) than in *B. brassicae* (9.38 s) ($P<0.01$) and was well correlated with the total pd durations ($r = 0.99$ and 0.94, for *A. gossypii* and *B. brassicae*, respectively) but apparently not with the duration of subphases α, β, or γ. Subphase δ(+ε) (equivalent to II-3) has convincingly been correlated with the acquisition of non-persistently transmitted viruses, but acquisition can occur during pd periods without pulses (Collar, 1996). Efficient aphid vectors for non-persistent viruses (*M. persicae* or *A. gossypii*) usually made longer II-3 (δ + ε) subphases than inefficient vectors [*Sitobion avenae* (Fabricius) and *Rhopalosiphum padi* (L.); Collar & Fereres, 1998]. Although subphase δ is apparently related to ingestion, the biological significance of the ε pulses remains unsolved. Possibly, the cibarial valve does not open until subphase δ and ingestion of cytosol might be passive, driven by the cell's turgor pressure.

CMV inoculation by interrupted pds

In complete pds, the subphase waveforms or their accurate starting times could not always be established unequivocally due to natural signal irregularities ('biological noise'); positive spikes and low frequency components interfered with the regular subphase waveforms. However, going forward and backward through the complete pd signal, zooming in and out as well as comparing full and R-EPGs, mostly allowed identification of subphases and starting times with some accuracy (see previous sections). In this CMV inoculation experiment, we used only the first pd within a probe, which often occurred so fast that optimal plant voltage adjustment (Figure 1) of the full EPG signal had not yet been achieved. This is normally needed to get a good signal quality in new recordings. If a pd waveform in the full EPG of an inoculation probe went out of scale and the concurrently recorded R-EPG did not provide enough details either, the recording had to be rejected. Also, with a good R-EPG signal available and a (partly) out of scale full EPG, it was not possible to detect pd periods. Subphase identification appeared much more difficult in interrupted inoculation pd waveforms than in complete pd waveforms. We mentioned the β–γ–δ similarity already in the foregoing sections. Although not common in *A. gossypii*, we carefully looked at both, full and R-EPGs to establish the occurrence of any subphase γ features before the interruption.

Results of inoculation success by viruliferous aphids interrupted after different pd subphases could only be established after signal analysis and virus detection in tests plants. After rejection of ambiguous EPG recordings from 110 aphids, recordings from 98 aphids could be used but only 61 of these were positively related to CMV-infected plants, either first test plant used for EPG recorded probes or second test plant used for the subsequent 24 h inoculation access period (IAP) without EPG recording (Table 1). Of these 61 viruliferous aphids, 39 (64%) had inoculated CMV successfully during the recorded probe whereas 22 (36%) had not. The inoculation success ratio (positive/all) was not significantly different ($P>0.05$) with more subphases in

Table 1 Inoculation results from interrupted pd waveforms after different subphases

A				B	Last pd subphase shown		
					α + β	γ	δ + ε
	Total	98		CMV negative	12	6	4
	Pos acquisition	61	62%	CMV positive	22	7	10
	Inoc. neg inoculation	22	36%	Inoc. success ratio (%)	64.7	53.8	71.4
	Inoc. pos inoculation	39	64%		χ^2	P	
				Overall	0.924	0.63	
				α+β vs. γ	0.469	0.49	
				α+β vs. δ(+ε)	0.202	0.65	
				γ vs. δ(+ε)	0.894	0.34	

P-values obtained according to a χ^2 test and to Fisher's exact test when expected values were lower than 5.
(A) Number of aphids (from 98 recordings of aphids) analysed. Pos acquisition: aphids viruliferous, i.e., test plant 1 and/or 2 infected. Inoc. neg, negative inoculation: test plant 1 not infected. Inoc. pos, positive inoculation: test plant 1 infected. (B) Number of CMV-infected and non-infected plants after each of the different subphases (α + β, γ, δ + ε).

the interrupted inoculation pd period (Table 1). We could not reliably distinguish subphase β in interrupted full EPG recordings so that we needed to lump α and β, and it was impossible to distinguish single or multiple waves of γ_i subphases in R-EPGs when pd waveforms had been interrupted before subphase γ. Inoculation results for complete pd periods required pooling of δ + ε subphases as well because we did not attempt to interrupt before ε and the number of aphids showing a clear ε pulses was very small (three and four for negative and positive CMV inoculation, respectively).

Thus, the first subphases α + β represent the major contribution to CMV inoculation, confirming earlier findings (Martin et al., 1997) that salivation during subphase II-1, i.e., the α + β equivalent, is responsible for release and inoculation of virions. On the other hand, we cannot exclude that virions are released before the first pd, during extracellular gelling or cannot be excluded completely during pathway. Such virion transfer, however, does not reach any suitable plant location for successful virus inoculation. We also cannot exclude the possibility that within a pd period, some minor salivation with virion release may occur during subphases γ_i, γ, δ, and ε, although the major salivation with inoculation occurs during subphase α + β. Any later virion release might be redundant and therefore difficult to demonstrate in CMV inoculation experiments such as ours. The role of the respective subphases in inoculation of other non-persistent and semi-persistent viruses is presently studied further (CSIC, Madrid, Spain). Our experiments do not indicate whether or not egestion (Harris & Harris, 2001) occurs during any pd subphase, although these and earlier results clearly demonstrate that salivation during subphase II-1 causes the non-persistent virus inoculation.

Conclusions

The intracellular punctures, reflected as pd waveforms in the EPG, include a number of waveform subphases and underlying activities which exceed those distinguished to date. The five new temporary subphases described here do not support the proposed subdivision made by Harris & Harris (2001), which was not based on any real signal analysis or experimental results. Also, the proposed division of subphase II-3 (Zhang et al., 2001) similar to our subphases δ and ε seems artificial, as our signal analysis suggests that the pulses occur superimposed on the continuous subphase δ waveforms rather than forming a separate subphase. Thus, we cannot support these earlier proposed subphase divisions.

Our results suggest one more or less continuous activity starting at subphase β and ending with subphase δ(+ε), mainly on the basis of pd waveforms in the full EPG by *B. brassicae* (Figure 2B), also occurring in the two other aphids, although less often. However, the biological meaning cannot be explained yet and needs further research. The 'intensity' of the emf-component may change, especially during subphase γ (II-2), as shown by the (pure) emf-recordings (cf., Figure 7A and B). Unequivocal distinction of all new subphases appeared only possible in a limited number of cases, in spite of serious attempts to use information from full EPG and concurrently recorded R-EPG signals. Although the γ_i subphase details were not shown in full EPGs, in R-EPGs the 'old subphases' could not or hardly be distinguished except subphase γ. This

subphase showed a high full/R-EPG synchrony and therefore it was equally well distinguished by both EPG circuits. Therefore, our conclusion is that recording full EPG and R-EPG signals side by side did not provide a better distinction or more accurate starting times of completed pd subphases.

The only advantage of concurrent full and R-EPG signals appeared when pd episodes were interrupted, which seems relevant only in transmission studies of non-circulative viruses (non-persistent or semi-persistent). Thus the R-EPG can be helpful to avoid misinterpretation of subphase β (late II-1) features as subphase γ (II-2). In other research applications of EPGs, however, the three 'old' subphases could be recognised reliably with only the full EPG signals available (DC EPG system). We, therefore, do not support the retention of this new subphase classification for future studies, and concurrent recording of full and R-EPGs cannot be recommended for routine monitoring for the majority of EPG applications. Recording full and R-EPGs side-by-side will double the time required for EPG analysis without substantial benefits. This confirms earlier conclusions drawn from full/R-EPG recordings of thrips EPGs (Kindt et al., 2006).

Our experiments have shown again that pd subphase α + β (II-1) represents the major contribution to CMV inoculation and the role of the later pd subphases seems insignificant. There is no reason to suppose that this is not also true for other non-persistently transmitted viruses.

Acknowledgements

This project has been funded by the Spanish government, Ministry of Education and Science grants SAB2005-0009 and AGL-2003-07532-C03-01. We also thank Maria Plaza for technical assistance and Glen Powell for critical comments and language corrections.

References

Backus EM & Bennett WH (2009) The AC–DC correlation monitor: new EPG design with flexible input resistors to detect both R and emf components for any piercing–sucking hemipteran. Journal of Insect Physiology 55: 869–884.

Chen J, Martin B, Rahbé Y & Fereres A (1997) Early intracellular punctures by two aphid species on near-isogenic melon lines with and without the virus aphid transmission (Vat) resistance gene. European Journal of Plant Pathology 103: 521–536.

Collar JL (1996) Dispersion del Virus Y de la Patata (PVY) en Plantas de Pimiento (*Capsicum annuum* L.) Tratadas con Diferentes Insecticidas. PhD Dissertation, Universidad Politécnica de Madrid, Spain.

Collar JL & Fereres A (1998) Nonpersistent virus transmission efficiency determined by aphid probing behavior during intracellular punctures. Environmental Entomology 27: 583–591.

Collar JL, Avilla C & Fereres A (1997) New correlations between aphid stylet paths and nonpersistent virus transmission. Environmental Entomology 26: 537–544.

Fereres A & Collar JL (2001) Analysis of noncirculative transmission by electrical penetration graphs. Virus-Insect-Plant Interactions (ed. by KF Harris, OP Smith & JE Duffus), pp. 87–109. Academic Press, London, UK.

Gray S & Gildow FE (2003) Luteovirus-aphid interactions. Annual Review of Phytopathology 41: 539–566.

Harris KF & Harris LJ (2001) Ingestion-egestion theory of cuticula-born virus transmission. Virus-Insect-Plant Interactions (ed. by KF Harris, OP Smith & JE Duffus), pp. 111–132. Academic Press, London, UK.

van Helden M & Tjallingii WF (2000) Experimental design and analysis in EPG experiments with emmphasis on plant resistance research. Principles and Applications of Electronic Monitoring and other Techniques in the Study of Homopteran Feeding Behavior (ed. by GP Walker & EA Backus),pp. 41–69. Entomological Society of America, Lanham, MD, USA.

Kindt F, Joosten NN & Tjallingii WF (2006) Electrical penetration graphs of thrips revised: combining DC- and AC-EPG signals. Journal of Insect Physiology 52: 1–10.

Martin B, Collar JL & Tjallingii WF (1997) Intracellular ingestion and salivation by aphids may cause the acquisition and inoculation of non-persistently transmitted plant viruses. Journal of General Virology 78: 2701–2705.

McLean DL & Kinsey MG (1964) A technique for electronically recording aphid feeding and salivation. Nature 202: 1358–1359.

McLean DL & Weigt WA Jr (1968) An electronic measuring system to record aphid salivation and ingestion. Annals of the Entomological Society of America 61: 180–185.

Pettersson J, Tjallingii WF & Hardie J (2007) Host-plant selection and feeding. Aphids as Crop Pests (ed. by HF van Emden & R Harrington),pp. 87–113. CABI, Wallingford, UK.

Powell G (1991) Cell membrane punctures during epidermal penetrations by aphids consequences for the transmission of two potyviruses. Annals of Applied Biology 119: 313–322.

Powell G (2005) Intracellular salivation is the aphid activity associated with inoculation of non-persistently transmitted viruses. Journal of General Virology 86: 469–472.

Powell G, Pirone T & Hardie J (1995) Aphid stylet activities during potyvirus acquisition from plants and an *in vitro* system that correlate with subsequent transmission. European Journal of Plant Pathology 101: 411–420.

Reese JC, Tjallingii WF, van Helden M & Prado E (2000) Waveform comparison among AC and DC electronic monitoring systems for aphid (Homoptera, Aphididae) feeding behavior. Principles and Applications of Electronic Monitoring and other Techniques in the Study of Homopteran Feeding Behavior (ed. by GP Walker & EA Backus),pp. 70–101. Entomological Society of America, Lanham, MD, USA.

Scheller HV & Shukle RH (1986) Feeding behavior and transmission of barley yellow dwarf virus by *Sitobion avenae* on oats. Entomologia Experimentalis et Applicata 40: 189–195.

Tjallingii WF (1985a) Electrical nature of recorded signals during stylet penetration by aphids. Entomologia Experimentalis et Applicata 38: 177–186.

Tjallingii WF (1985b) Membrane potentials as an indication for plant cell penetration by aphid stylets. Entomologia Experimentalis et Applicata 38: 187–193.

Tjallingii WF (1988) Electrical recording of stylet penetration activities. Aphids, their Biology, Natural Enemies and Control, vol. 2B (ed. by AK Minks & P Harrewijn), pp. 95–108. Elsevier, Amsterdam, The Netherlands.

Tjallingii WF (2000) Comparison of AC and DC systems for electronic monitoring of stylet penetration activities by homopterans. Principles and Applications of Electronic Monitoring and other Techniques in the Study of Homopteran Feeding Behavior (ed. by GP Walker & EA Backus),pp. 41–69. Entomological Society of America, Lanham, MD, USA.

Tjallingii WF & Esch TH (1993) Fine structure of aphid stylet routes in plant tissues in correlation with EPG signals. Physiological Entomology 18: 317–328.

Tjallingii WF & Gabrys B (1999) Anomalous stylet punctures of phloem sieve elements by aphids. Entomologia Experimentalis et Applicata 91: 97–103.

Uzest M, Gargani D, Drucker M, Hebrard E & Garzo E et al. (2007) A protein key to plant virus transmission at the tip of the insect vector stylet. Proceedings of the National Academy of Sciences of the USA 104: 17959–17964.

Walker GP (2000) A beginners's guide to electronic monitoring of homopteran probing behavior. Principles and Applications of Electronic Monitoring and other Techniques in the Study of Homopteran Feeding Behavior (ed. by GP Walker & EA Backus),pp. 41–69. Entomological Society of America, Lanham, MD, USA.

Zhang PF, Chen JQ, Zhang X, Wang B & Jiang QF (2001) The feeding behavior and the acquisition of CMV by the cotton aphid *Aphis gossypii*. Acta Entomologica Sinica 44: 395–401.